厚生労働科学研究費補助金（障害者対策総合研究事業）

分担研究報告書

筋ジストロフィー患者の尿中プロスタグランジンD2代謝物の定量分析

研究分担者　竹内　敦子　神戸薬科大学　准教授

研究要旨

Duchenne型筋ジストロフィー（Duchennne muscular dystrophy ：DMD）は進行性の筋萎縮を呈し，ほぼ20歳代に心不全または呼吸不全により死亡する極めて重篤な遺伝性疾患である。本疾患は，原因遺伝子であるジストロフィン遺伝子の変異により，筋の細胞膜形成に関与するジストロフィンタンパク質が欠損し，筋細胞が壊れるため発症する。近年，DMD 患者の壊れかけた筋肉では炎症やアレルギーなどに関与するプロスタグランジンD2（PGD2）合成酵素の発現が亢進していることが明らかとなった。これまでに，PGD2の尿中代謝物 である tetranor-PGDM（PGDM）のLC-MS/MSを用いる定量法を確立した。DMD患者、BMD患者および健常者について測定したところ、DMDの病状診断に有効である可能性が示唆された。そこで、他の筋疾患患者の尿中PGDMを測定したところ、疾患により差が認められた。

A．研究目的

Duchenne 型筋ジストロフィー(Duchennne muscular dystrophy ： DMD)は進行性の筋萎縮を呈し，極めて重篤な遺伝性疾患である。本疾患は，原因遺伝子であるジストロフィン遺伝子のエクソン欠失および重複等の変異により，筋の細胞膜形成に関与するジストロフィンタンパク質が欠損する遺伝性筋疾患である。人種に関係なく出生男子約3500人に1人の割合で発症する。

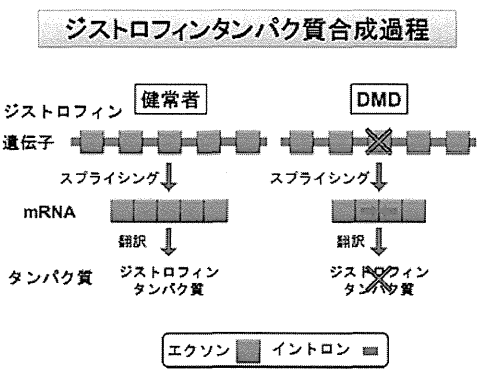

DMD患者は4～5歳時に筋力低下を認め，年齢と共に筋委縮が進行し，10～12歳時には歩行能を失う。そして心筋あるいは呼吸筋の障害が出現し，心不全あるいは呼吸不全により，多くは20歳代で死に至る。

近年，DMD 患者の壊れかけた筋肉では，炎症やアレルギーなどに関与するプロスタグランジンD2合成酵素（PGD2 synthase ： PGDS)の発現が亢進していることが明らかとなった。したがって、DMDの病状診断に PGD2 の尿中代謝物である tetranor-PGDM（PGDM）濃度の定量が有効であるとの考えに至った。

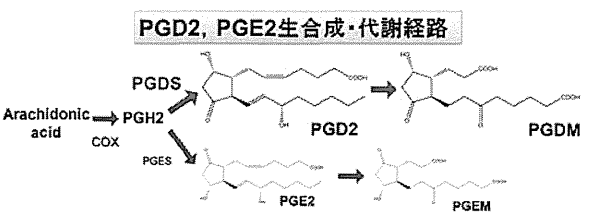

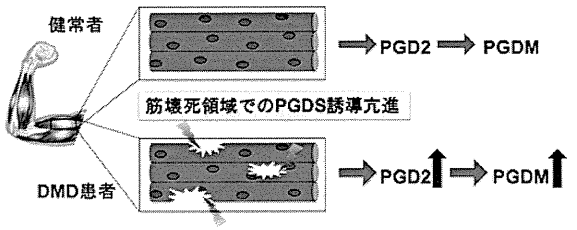

B．研究方法

1）対象

2～55 歳の患者 1,003 検体および 2～14 歳の健常者 116 検体、健常成人 86 検体を対象とした。

各種筋疾患患者の内訳は、DMD、BMD、γ-サルコグリカノパチー、ラミノパチー、先天性ミオパチー、B-ジストログリカン異常などである。

また、尿中 PGDM 濃度の日内変動を調べたところ、概して早朝に低く、日中に高い傾向が見られたことから、早朝一番尿を採取した。

2）測定用試料の調製および LC-MS/MS による定量

患者および健常者の尿 0.4ml に純水Ｂ0.5ml を加え、さらに内標準物質(tetranor-PGDM-d6)を加えて混和したのち，1N HCl で pH3 程度に調整した。次に固相抽出カラム Sep-Pak Vac を用いて抽出した。この抽出液を窒素ガスで濃縮乾固したのち、10%アセトニトリル 100μl で再溶解して測定用試料とした。検量線作成のために内標準物質を加えた各濃度の標準試料についても同様に作成した。標準試料・測定用試料を API3000 LC-MS/MS system に適用し，最適条件におけるプリカーサーおよびプロダクトイオンを検討した後，SRM（Selected Reaction Monitoring）法で測定した。PGDM と内標準物質とのピーク面積比を用いて定量値を算出した。また，比色定量によりクレアチニンを定量し，補正した。

C．研究結果

2～55 歳の患者から採取した早朝一番尿 1,003 検体中の PGDM を測定したところ、健常者の尿に比べ、高かった。

各種筋疾患患者のうち、DMD と BMD を比較したところ、尿中 PGDM は DMD の方が有意に高かった。

DMD、BMD、γ-サルコグリカノパチー、ラミノパチー、先天性ミオパチー、B-ジストログリカン異常他の筋疾患の尿中 PGDM を測定したところ、疾患により差が認められた。著しく高値を示す疾患があったが、検体数が少ないため今後の課題とし、検体数を増やして検討する必要がある。

D．考察

DMD 患者および健常者について測定したところ、DMD の病状診断に有効である可能性が示唆された。また、他の筋疾患患者の尿中 PGDM を測定したところ、疾患により差が認められた。以上の結果より、治療効果の判定に応用可能であるとが考えられた。

今後は、DMD 患者に薬による治療を行い、その効果の判定に応用していく予定である。

E．結論

尿中 PGDM は、健常者＜BMD 患者＜DMD 患者の順に高かったことから、DMD の病状診断に有効であることが明らかとなった。

F．研究発表

1．論文発表

なし

2．学会発表

1) Taku Nakagawa, Atsuko Takeuchi, Ryohei Kakiuchi, Tomoko Lee, Mariko Yagi, Hiroyuki Awano, Kazumoto Iijima, Yasuhiro Takeshima, Yoshihiro Urade, Masafumi Matsuo
"A prostaglandin D2 metabolite is elevated in the urine samples of patients with Duchenne muscular dystrophy" 18th International WMS Congress (2013. 10.1-5 Asilomar, California, USA)

2) 松尾　雅文，裏出　良博，竹内　敦子
「デュシェンヌ型筋ジストロフィーの尿中プロスタグランジン代謝産物解析」第40回BMSコ

ンファレンス（2013.7.9　宮崎）

3) 竹内　敦子，裏出　良博，松尾　雅文
「LC-MS/MSによるDuchenne型筋ジストロフィー患者の尿中プロスタグランジンD2代謝物の定量」第40回BMSコンファレンス（2013.7.9　宮崎）

4) 柳下　沙絢，竹内　敦子，中川　卓，竹島　泰弘，裏出　良博，松尾　雅文
「デュシェンヌ型筋ジストロフィー患者尿中プロスタグランジンD2代謝物濃度」第61回質量分析総合討論会（2013.9.10　つくば）

5) Atsuko Takeuchi
" LC-MS/MS quantification of a prostaglandin D2 metabolite in the urine of Duchenne muscular dystrophy patients"
Japan-Vietnam joint research meeting on Duchenne muscular dystrophy（2014.2.26 Hanoi, Vietnam）

G．知的財産権の出願・登録状況
なし

厚生労働科学研究費補助金（障害者対策総合研究事業）
分担研究報告書

動物モデルを用いた筋壊死と尿中代謝物の相関の実証
（心筋症モデルでの心筋壊死と薬物投与効果および尿中代謝物の関係）

分担研究者：岩田裕子　国立循環器病研究センター研究所分子生理部　室長

【研究要旨】
拡張型心筋症は、その発症機序が不明であり予後も不良であることから、新たな治療法の確立が求められている。分担研究者は、Duchenne 型筋ジストロフィーにおいて骨格筋における病態進行とプロスタグランジンD_2 産生が相関するとの知見に基づき、心筋組織においても同様に、筋壊死に伴う病態進行とPGD_2 産生の亢進が関連している可能性を検証した。また、拡張型心筋症モデルハムスターにHPGDS 阻害薬を投与することにより、拡張型心筋症病態の進行が抑制される可能性が示された。

A. 研究目的

拡張型心筋症は、その発症機序が不明であり予後も不良であることから、新たな治療法の確立が求められている。これまでに、Duchenne型筋ジストロフィーの病態進行と造血器型PGD合成酵素（HPGDS）によるプロスタグランジン（PG）D_2産生が相関することが強く示唆されている。そこで研究分担者は、心筋組織においても同様に、筋壊死に伴う病態進行とPGD_2産生の亢進が関連している可能性を検証するため、拡張型心筋症のモデル動物（ハムスター、マウス）を用いた解析を行った。

B. 研究方法

δ- sarcoglycan を欠損した拡張型心筋症モデルハムスターを用いた。対照として、同週齢の野生型動物を用いた。10 週齢の心筋症ハムスターにHPGDS 阻害薬(30mg/kg/day)または溶媒(PBS)を 3 週間、皮下投与し、組織の繊維化と心機能を指標に、薬効を評価した。繊維化はマッソントリクローム染色により確認した。心機能は、小動物用超音波高解像度イメージングシステム(VISUALSONICS)を用い

て、麻酔下で非侵襲的に評価した。

PGD_2産生量の変動を評価するため、代謝ケージを用いて暗期（12時間）に採尿し、PGD_2の尿中安定代謝物 11,15-Dioxo-9-hydroxy-2, 3, 4, 5-tetranorprostan-1, 20-dioic acid (tetranor-PGDM)を液体クロマトグラフィー・タンデムマススペクトロメトリーを用いて測定した（LC: 資生堂、MS/MS: AB Sciex)。

（倫理面への配慮）

実験動物を用いる研究については、国立循環器病研究センター動物実験指針に準拠して実施した。本研究計画は動物実験委員会の承認を得ている。また、麻酔使用等により動物愛護上の倫理的配慮を行い、適切な環境のもとで飼育管理を行った。

C. 研究結果

拡張型心筋症モデルハムスターでは、野生型動物に比べ、心臓組織でのHPGDS蛋白質の発現量が2・5倍程度増加していた。また、両者から単離した心筋細胞の比較においてもHPGDSの発現増加が示された。心臓及び心筋細胞を用いた免疫染色の結果から、HPGDSの介在板近傍への強い集積が認められた。これらの知見は、心筋症病態の進行に伴い、同週齢の野生型動物に比べ、尿中 tetranor-PGDM 量が高値を示すことと一致する。

拡張型心筋症モデルハムスターへの HPGDS 阻害薬の投与(30mg/kg/day)により、尿中tetranor-PGDMが減少することを確認した。心臓組織の繊維化を定量したところ、溶媒投与群に比べて、HPGDS阻害薬の投与群では、繊維化の進行に抑制傾向が観察された。小動物用超音波高解像度イメージングシステムにより、心機能を評価したところ、溶媒投与群に比べ、HPGDS阻害薬の投与群では、左室内径短縮率(%FS)の低下に抑制傾向が見られた。

D. 考察

拡張型心筋症モデルハムスターにおいて、尿中tetranor-PGDM量が高値を示す症例が認められた。そこで、HPGDS阻害薬投与による薬効評価を行ったところ、心臓組織の繊維化進行、および心機能の低下を軽減させる傾向が示された。したがって、HPGDSにより産生されたPGD_2がハムスターの拡張型心筋症病態の進行に重要な役割を持つ可能性が示された。

拡張型心筋症のモデルマウスでも、尿中tetranor-PGDM量が高値を示すことから、今後これらの動物モデルを用いて、心筋組織におけるPGD_2産生と病態進行の関連性を明らかにする

必要がある。

拡張型心筋症は、その発症機序が不明であり予後も不良であることから、新たな治療法の確立が求められている。HPGDS 阻害薬の投与実験を行うことで、新規治療法開発の可能性を検証できる。また、治療対象の決定や薬剤効果を評価できるマーカーが必要であるが、尿中の安定代謝物であるtetranor-PGDMがその候補として期待される。

E. 結論

HPGDS 阻害薬が拡張型心筋症の病態進行を抑制できる可能性が示唆された。

F. 研究発表

1．論文発表

1) Maekawa K, Hirayama A, Iwata Y, Tajima Y, Nishimaki-Mogami T, Sugawara S, Ueno N, Abe H, Ishikawa M, Murayama M, Matsuzawa Y, Nakanishi H, Ikeda K, Arita M, Taguchi R, Minamino N, Wakabayashi S, Soga T, Saito Y. Global metabolic analysis of heart tissue in a hamster model for dilated cardiomyopathy. ***J. Mol. Cell Cardiol.***, 59: 76-85,2013

2) Iwata Y, Ohtake H, Suzuki O, Matsuda J, Komamura K, Wakabayashi S. Blockade of sarcolemmal TRPV2 accumulation inhibits progression of dilated cardiomyopathy. ***Cardiovas. Res.***, 99: 760-768, 2013

2．学会発表

1) 第 86 回日本生化学会大会
(2013 年 9 月 11-13 日、横浜)
鎌内慎也、岩田裕子、若林繁夫
「Prostaglandin D_2 metabolites are elevated in the urine of animal models of dilated cardiomyopathy」

G. 知的財産権の出願・登録条件

1．特許取得

なし

2．実用新案登録

なし

3．その他

なし

研究成果の刊行に関する一覧表

学会発表

発表者氏名	演題名	学会名	発行年
Yoshiro Urade	Use of protein crystal growth technology in space to discover and develop therapeutic candidates for Duchenne muscular dystrophy	2nd Annual ISS research and development conference	2013
Atsuko Takeuchi	LC-MS/MS quantification of a prostaglandin D2 metabolite in the urine of Duchenne muscular dystrophy patients" Japan-Vietnam joint research meeting on Duchenne muscular dystrophy	Hanoi, Vietnam	2013
Yoshihiro Urade	Development of drugs used for therapy of Duchenne muscular dystrophy : Inhibitors of hemato-poietic prostaglandin D synthase" Japan-Vietnam joint research meeting on Duchenne muscular dystrophy	Hanoi, Vietnam	2013
松尾雅文，裏出良博，竹内敦子	デュシェンヌ型筋ジストロフィーの尿中プロスタグランジン代謝産物解析」第 40 回 BMS コンファレンス	第 40 回 BMS コンファレンス(宮崎)	2013
竹内敦子，裏出良博，松尾雅文	「LC-MS/MS による Duchenne 型筋ジストロフィー患者の尿中プロスタグランジン D2 代謝物の定量」第 40 回 BMS コンファレンス	第 40 回 BMS コンファレンス(宮崎)	2013

柳下沙絢，竹内敦子，中川卓，竹島泰弘，裏出良博，松尾雅文	デュシェンヌ型筋ジストロフィー患者尿中プロスタグランジン D2 代謝物濃度	第 61 回質量分析総合討論会（つくば）	2013
裏出良博、中川　卓、竹内敦子、垣内涼平、Tomoko Lee、八木麻里子、粟野宏之、飯島一誠、竹島泰弘、松尾雅文、有竹浩介	デュシェンヌ型筋ジストロフィーの新規病態マーカーとしての尿中 PGD2 代謝物」	第 86 回日本生化学会大会	2013
有竹浩介、田中克尚、鈴木比佐子、三好和久、林　勧生、佐々木英治、裏出良博	Effect of a highly selective inhibitor for hematopoietic prostaglandin D synthase on an experimental model of Duchenne muscular dystrophy	第 86 回日本生化学会大会	2013
T.Nakagawa; A.Takeuchi; R.Kakiuchi; T.Lee; M.Yagi; H.Awano; K.Iijima; Y.Takeshima; Y.Urade; M.Mtsuo.	A prostaglandin D2 metabolite is elevated in the urine samples of patients with Duchenne muscular dystrophy	18th International WMS Congress (CA, USA)	2013.10.3
Masafumi Matsuo	Mutations in the dystrophin gene	日本-ベトナム Duchenne 型筋ジストロフィー関する共同研究会議	2014.8.26
Masafumi Matsuo	DMD treatment : overview	日本-ベトナム Duchenne 型筋ジストロフィー関する共同研究会議	2014.2.26

雑誌

発表者氏名	論文タイトル名	発表誌名	巻号	ページ	出版年
Nakagawa T, Takeuchi A, Kakiuchi R, Lee T, Yagi M, Awano H, Iijima K, Takeshima Y, Urade Y, Matsuo M	A prostaglandin D_2 metabolite is elevated in the urine of Duchenne muscular dystrophy patients and increases further from 8years old.	***Clin. Chim. Acta.***	423	10-14	2013
Maekawa K, Hirayama A, Iwata Y, Tajima Y, Nishimaki-Mogami T, Sugawara S, Ueno N, Abe H, Ishikawa M, Murayama M, Matsuzawa Y, Nakanishi H, Ikesa K, Arita M, Taguchi R, Minamino N, Wakabayashi S, Soga T, Saito Y	Global metabolomic analysis of heart tissue in a hamster model for dilated cardiomyopathy.	***J Mol Cell Cardiol***	59	76-85	2013
Iwata Y, Ohtake H, Suzuki O, Matsuda J, Komamura K, Wakabayashi S	Blockade of sarcolemmal TRPV2 accumulation inhibits progression of dilated cardiomyopathy.	***Cardiovasc Res***	99(4)	760-768	2013
Sarashina H, Tsubosaka, Y, Omori K, Aritake K, Nakagawa M, Hori M, Hirai H, Nakamura M, Narumiya S, Urade Y, Ozaki H, Murata T	Opposing immunomodulatory roles prostaglandin D_2 during the progression of skin inflammation	***J Immunol***	192	459-465	2014

Taketomi Y, Ueno N, Kojima T, Sato H, Murase R, Yamamoto K, Tanaka S, Sakanaka M, Nakamura M, Nishito Y, Kawana M, Kambe N, Ikeda K, Taguchi R, Nakamizo S, Kabashima K, Gelb MH, Arita M, Yokomizo T, Nakamura M, Watanabe K, Hirai H, Nakamura M, Okayama Y, Ra C, Aritake K, Urade Y, Morimoto K, Sugimoto Y, Shimizu T, Narumiya S, Hara S, Murakami M.	Mast cell maturation is driven via a grouop III Phospholipase A_2-Prostaglandin D_2-DPI receptor paracrine axis	***Nat Immunol***	14(6)	554-563	2013
Murata, T., Aritake, K., Tsubosaka, Y., Maruyama, T., Nakagawa, T., Hori, M., Hirai, H., Nakamura, M. Narumiya, S., Urade, Y., Ozaki, H.	Anti-inflammatory role of PGD_2 in acute lung inflammation and therapeutic application of its signal enhancement	***Proc Natl Acad Sci U S A***	110 (13)	5205-10	2013
Izumi Y1, Aritake K, Urade Y, Fukusaki E.	Practical evaluation of liquid chromatography/tandem mass spectrometry and enzyme immunoassay method for the accurate quantitative analysis of prostaglandins.	***J Biosci Bioeng***		In press	2014

Clinica Chimica Acta 423 (2013) 10–14

Contents lists available at SciVerse ScienceDirect

Clinica Chimica Acta

journal homepage: www.elsevier.com/locate/clinchim

A prostaglandin D_2 metabolite is elevated in the urine of Duchenne muscular dystrophy patients and increases further from 8 years old

Taku Nakagawa [a], Atsuko Takeuchi [b], Ryohei Kakiuchi [b], Tomoko Lee [a], Mariko Yagi [a], Hiroyuki Awano [a], Kazumoto Iijima [a], Yasuhiro Takeshima [a], Yoshihiro Urade [c], Masafumi Matsuo [d,*]

[a] Department of Pediatrics, Graduate School of Medicine, Kobe University, Chuo, Kobe 6500017, Japan
[b] Kobe Pharmaceutical University, Higashinada, Kobe 6588558, Japan
[c] Department of Molecular Behavioral Biology, Osaka Bioscience Institute, Suita, Osaka 5650874, Japan
[d] Department of Medical Rehabilitation, Faculty of Rehabilitation, Kobegakuin University, Nishi, Kobe 6512180, Japan

ARTICLE INFO

Article history:
Received 25 January 2013
Received in revised form 27 March 2013
Accepted 27 March 2013
Available online 19 April 2013

Keywords:
Tetranor PGDM
Muscle wasting
Inflammation

ABSTRACT

Background: Duchenne muscular dystrophy (DMD) is a progressive muscle wasting disease caused by muscle dystrophin deficiency. Downstream of the primary dystrophin deficiency is not well elucidated. Here, the hypothesis that prostaglandin D_2 (PGD_2)-mediated inflammation is involved in the pathology of DMD was examined by measuring tetranor PGDM, a major PGD_2 metabolite, in urine of DMD patients.
Methods: We measured tetranor PGDM in urine using LC–MS/MS. First morning urine samples were collected from genetically confirmed DMD patients and age-matched healthy controls aged 4 to 15 y.
Results: The urinary tetranor PGDM concentration was 3.08 ± 0.15 and 6.90 ± 0.35 ng/mg creatinine (mean ± SE) in 79 control and 191 DMD samples, respectively. The mean concentration was approximately 2.2-times higher in DMD patients than in controls ($p < 0.05$). Remarkably, urinary tetranor PGDM concentrations in DMD patients showed chronological changes: it stayed nearly 1.5 times higher than in controls until 7 y but surged at the age of 8 y to a significantly higher concentration.
Conclusion: Urinary tetranor PGDM concentrations were shown to be increased in DMD patients and became higher with advancing age. It was indicated that PGD_2-mediated inflammation plays a role in the pathology of DMD.

1. Introduction

Duchenne muscular dystrophy (DMD; OMIM #310200) is the most common inherited muscle disease, affecting one in every 3500 male births and shows progressive muscle wasting resulting in early death. DMD is characterized by muscle dystrophin deficiency caused by mutations in the *dystrophin* gene, which is the largest human gene consisting of 79 exons. DMD patients all carry disastrous mutations in the *dystrophin* gene, such as frameshift or nonsense mutations [1,2]. However, there is some clinical heterogeneity among DMD patients [3,4] and intrafamilial differences have been observed in patients with an identical dystrophin mutation [5]. Dystrophin is a critical member of the dystrophin glycoprotein complex that creates a direct link between the intracellular cytoskeleton and the extracellular matrix of skeletal muscle. The loss of this connection leaves the muscle fibers susceptible to damage resulting in continuous rounds of muscle degeneration/regeneration.

DMD has been classically considered stereotyped in its clinical presentation, evolution, and severity [6–8]. In a minimal disability stage children are without symptoms or with minimal weakness. In the moderate disability stage, patients are impaired in running and climbing stairs. In the severe disability stage, patients are still ambulant but become increasingly handicapped in their physical activities. In the non-ambulant stage that starts before age 12 y, the children are bed-ridden or wheelchair-bound. This progression process has not been totally explained by a primary loss of dystrophin. Inflammatory and immune responses initiated by aberrant signaling in dystrophic muscle have been considered contributors to disease pathogenesis [9].

Prostaglandin (PG) D_2 (PGD_2) has been implicated in both the development and resolution of inflammation. PGD_2 is synthesized by PGD synthase (PGDS) from PGH_2 that is produced from arachidonic acid by the action of cyclooxygenase and 2 PGDS have been disclosed; lipocalin-type PGDS and hematopoietic PGDS (HPGDS)[10,11]. HPGDS in skeletal muscles was found immunohistochemically stained in some of DMD patients but not in controls [12]. This indicated that the inflammatory mediator PGD_2 plays a role in DMD pathology. However, detailed time-course studies of PGD_2 metabolism in DMD patients are incomplete. Recently, urinary 11,15-dioxo-9α-hydroxy-,2,3,4,5-

* Corresponding author at: Department of Medical Rehabilitation, Faculty of Rehabilitation, Kobegakuin University, 518 Arise, Ikawadani, Nishi, Kobe 651-2180, Japan. Tel./fax: +81 78 974 6194.
E-mail address: mmatsuo@reha.kobegakuin.ac.jp (M. Matsuo).

0009-8981/$ – see front matter © 2013 Elsevier B.V. All rights reserved.
http://dx.doi.org/10.1016/j.cca.2013.03.031

tetranorprostan-1,20-dioic acid (tetranor PGDM) was shown to be a major urinary metabolite of PGD_2 and to reflect its biosynthesis [13].

2. Materials and methods

2.1. Patients

More than 400 DMD patients were referred to the DMD specialist clinic at Kobe University Hospital (Kobe, Japan). Patients were regularly checked for their clinical findings. The causative mutation in the *dystrophin* gene was identified in each case [1]. When corticosteroid use was indicated, predonine was prescribed at 0.5 mg/kg on alternate days. However, fewer than one fifth of patients received corticosteroid therapy in our clinic. One hundred seventeen DMD patients from 4 to 15 y were enrolled in this study and their first morning urines were obtained at 191 points. Age matched 71 male controls were recruited from healthy relatives or volunteers and first morning urine were obtained at 79 points. Two samplings from 1 patient were done at least 6 months separated. Information concerning the clinical condition of the patients and controls was obtained from their parents and hospital records, respectively. Voluntary urine samples or first morning urine samples were collected. Urine samples were stored at −20 °C until analysis. The protocols used in this study were approved by the ethics committee of Kobe University School of Medicine. All urine analysis was conducted after obtaining informed consent from the patients' parents.

2.2. Measurement of urinary tetranor PGDM concentration using mass spectrometry

The urine samples (0.4 ml) diluted with 0.5 ml of water were acidified by the addition of 1 mol/l HCl (final pH ~ 3) and 50 μl (5 ng) of d6-tetranor PGDM and 9,15-dioxo-11α-hydroxy-,2,3,4,5-tetranorprostan-1,20-dioic acid (tetranor PGEM) (Cayman Chemical, Ann Arbor, MI) was added as an internal standard. The mixtures were purified by solid-phase extraction using Sep-Pak Vac 3 cc cartridges (Waters Corp., Milford, MA). The cartridges were pre-conditioned with 3 ml of ethanol and equilibrated with 3 ml of water. The urine sample was applied to the cartridge, which was washed with 6 ml of 5% (v/v) acetonitrile in and then with 6 ml of n-hexane. The analyte and internal standard were eluted from the cartridge with 3 ml of ethyl acetate. The eluate was collected and dried under vacuum. The resulting residue was reconstituted in 100 μl of 10% (v/v) acetonitrile. The sample solution (20 μl) containing tetranor PGDM and tetranor PGEM was then introduced into an API3000 LC–MS/MS system (Applied Biosystems, Foster City, CA) equipped with an electrospray (Turbospray) interface. The HPLC column was a 150 × 2.1-mm i.d. Inertsil ODS-3 (GL Sciences, Tokyo, Japan). LC separation was carried out using a mobile phase consisting of 0.01% (v/v) acetic acid (solvent A) and acetonitrile (solvent B). The following gradient was employed at a flow rate of 250 μl/min: initial (2 min) at 10:95 (A:B); 24 min at 30:70, 27 min at 70:30. The LC–MS/MS was operated in the negative ion mode. The urinary tetranor PGDM was measured in the selected reaction monitoring mode. The transitions monitored were *m/z* 327–143 for the endogenous material and *m/z* 333–149 for the internal standard. The scan time was 250 ms.

The self-prepared samples were used to document the specificity of this method. The linearity of standard calibration curve was examined by analysis of seven concentrations (0.125, 0.250, 0.625, 1.25, 2.50, 6.25 and 12.5 ng/ml). The limit of quantitation defined as the lowest concentration on the calibration curve could be determined with 75–125% of accuracy and CVs < 20%, and the limit of detection was determined at a S/N of 3. The recovery was obtained by experiments using spiked blank matrix with mutually independent replicates at three concentrations of tPGDM (2.50, 6.25 and 12.5 ng/ml). Ten measurements were performed at each of the above 3 concentrations. The intra-day CV of this method was examined using 10 parallel samples at 3 concentrations (2.50, 6.25 and 12.5 ng/ml) prepared as described above. All samples were analyzed on the same day together with the daily calibration; the accuracy and precision were determined at each concentration. Acceptance criteria defined as precision should not exceed 15%, while accuracy should be within 100 ± 15% at each concentration. Acetonitrile (HPLC grade), ethanol, n-hexane, ethyl acetate, and all other chemicals were from Wako Pure Chemical Industries Ltd. (Osaka, Japan).

2.3. Creatinine measurements

Urinary creatinine concentration was measured using a creatinine measurement kit (Wako Pure Chemical Industries Ltd.).

2.4. Statistical analysis

Group difference between DMD patients and healthy children was analyzed using *t*-tests or 2-way analysis of variance in GraphPad Prism 5 (GraphPad Software, Inc., La Jolla, CA). Statistical significance was set at $p < 0.05$.

3. Results

Tetranor PGDM in urine samples was determined in a selected ion monitoring mode by LC–MS/MS. The monitored product ion peaks of tetranor PGDM and tetranor PGEM were clearly separated in the mass chromatogram with each single peak but no interference peaks. The retention time of these peaks of urine samples matched with that of controls (Fig. 1). The concentration of tetranor PGDM was quantitated

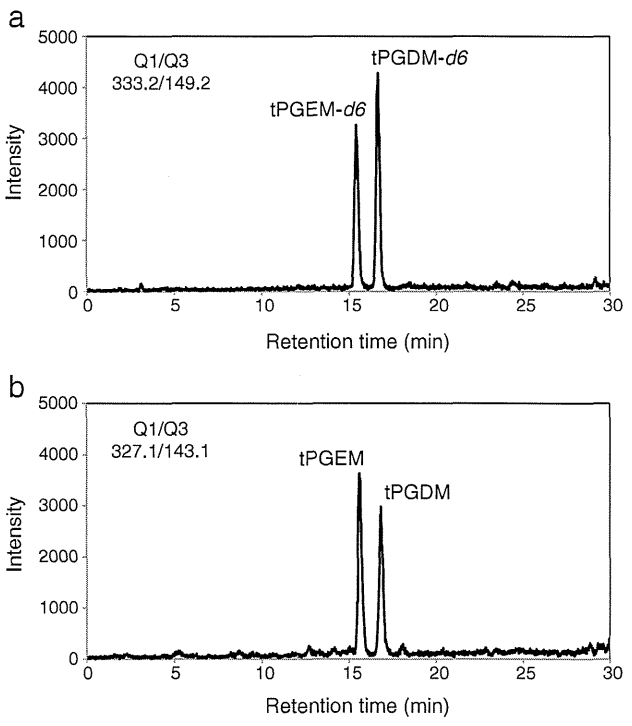

Fig. 1. LC–MS/MS chromatograms. Representative chromatograms of d6-teteranor PGDM and d6-tetranor PGEM (a) and endogenous compounds in urine (b). The first-order MS (Q1) analysis was conducted using negative ion scanning mode to ascertain that the precursor ion peak of d6-tetranor PGDM and tetranor PGDM was $[M-H]^-$ and M-1 of these compounds was 332.2 and 327.1, respectively. The second-order MS (Q2) analysis was done after the collision of precursor ion of the respective PGDM with $[M-H]^-$. Through adjustment of cone voltage and impact energy, the second-order mass chromatogram was obtained, and is shown. The ion transitions (Q1/Q3) of *m/z* 332.2/149.2 and 327.1/143.1 were used to analyze quantitatively and qualitatively, respectively.

using the peak area ratios of tetranor PGDM to d6-tetranor PGDM, on the basis of the calibration curve. The calibration curve was linear in the concentration range of 0.125–12.5 ng/ml (1/x weighting, $y = 0.072x + 0.00503$, $r = 0.997$). The lower limit of quantification reached 0.125 ng/ml. The intra- and the inter-day precision were less than 5.5% and 8.5%, respectively. The current LC–MS/MS method was validated as simple, sensitive, and accurate.

Urinary tetranor PGDM concentrations of DMD patients were determined in samples obtained at voluntary urination. The concentration fluctuated during the day but the first morning urine showed the lowest daytime concentration in all the examined paired samples (data not shown). Therefore, we used the first morning urine for further analyses, as has been suggested for adults [14]. Urine samples were obtained at 191 points from 117 DMD patients aged from 4 to 15 y and 79 points from 71 age-matched healthy children (Fig. 2a). In controls, the concentration of tetranor PGDM was 3.08 ± 0.15 ng/mg creatinine (mean ± SE), with a range of 1.23 to 7.08 ng/mg creatinine. In contrast, the concentration in DMD patients was 6.90 ± 0.35 ng/mg creatinine (range, 0.38 to 26.46 ng/mg creatinine). The mean concentration of tetranor PGDM in DMD patients was approximately 2.2-times higher than that in controls ($p < 0.0001$).

Corticosteroids are administered to DMD patients even though the mechanism of action is unknown [15]. One report suggested that the anti-inflammatory effect of corticosteroids is due to the suppression of prostaglandin-related inflammation [16]. Therefore, we examined whether corticosteroid administration affected the urinary excretion of tetranor PGDM. The average urinary excretion of tetranor PGDM was 5.44 ± 0.81 ($n = 28$) and 7.15 ± 0.38 ($n = 163$) ng/mg creatinine in DMD patients with and without corticosteroid therapy, respectively (Fig. 2b). No significant difference ($p = 0.078$) was found. This indicates that the benefit of our corticosteroid treatment is not observed.

To examine chronological changes, we plotted urinary tetranor PGDM concentrations against the age of the patients (Fig. 3a). The concentration in controls did not change greatly by age. In DMD patients, the tetranor PGDM concentrations were higher at younger ages (4–7 y) than in controls. Remarkably, they surged still higher from age 8 to 9 y, the beginning of the non-ambulant stage, and stayed in high concentration thereafter. Urinary tetranor PGDM was significantly higher in the older age DMD group (age 8–15 y) than in the younger age group (age 4–7 y) (Fig. 3b). In contrast, urinary tetranor PGDM was significantly lower in the older age control group (age 8–15 y) than in the younger age group (age 4–7 y) (Fig. 3b). Our results indicated high production of PGD_2 in DMD patients and suggested a role of PGD_2 in DMD pathology, especially the older DMD patients.

4. Discussion

We established a way to quantitate urinary PGDM using LC–MS/MS without a treatment of urine sample with methoxyamine (Fig. 1). Our quantitation way became suitable for clinical application by avoiding a time- and cost-consuming methoxyamine modification that has been employed [13]. It was found that urinary concentrations of tetranor PGDM were approximately 2.2-times higher in DMD patients than in controls (Fig. 2). Furthermore, it was first shown that urinary tetranor PGDM concentrations in DMD patients chronologically fluctuated (Fig. 2). It was remarkable that concentrations of urinary tetranor PGD_2 increased still further from the age of 8 y. Since the concentration of urinary tetranor PGDM has been reported to reflect the amount of PGD_2 in the body and ultimately reflect the activity of HPGDS [13], our findings indicated high HPGDS activity in the body of DMD patients. Immunohistochemical examination of HPGDS in biopsied skeletal muscle disclosed HPGDS-positive necrotic muscle fibers from DMD patients and myositis patients [12]. However, HPGDS was not stained in skeletal muscles of the control and Fukuyama-type muscular dystrophy [12]. Urinary excretion concentration of tetranor PGDM in DMD patients (Fig. 2) implied a 2.2-times increase in HPGDS. Our findings were also consistent with those of a murine study, in which the urinary concentration of tetranor PGDM was approximately 3-times higher in *mdx* mice than in wild-type mice [16]. This indicates that similar pathogenic mechanisms caused by primary dystrophin deficiency occur in both human and mouse. PGD_2 is considered an important molecule in the pathology of DMD.

Urinary tetranor PGDM has been shown to be increased in adults with inflammatory conditions such as chronic obstructive pulmonary disease, asthma, and amyotrophic lateral sclerosis, and PGD_2 is considered a mediator of inflammation in these conditions [13,14,17,18]. Therefore, increased urinary concentrations of tetranor PGDM in DMD suggested that PGD_2-mediated inflammation plays a role in the pathology of DMD. This finding may pave the way towards understanding the pathogenesis of DMD. However, it was questioned why urinary tetranor PGDM concentration increased by aging. As HPGDS is expressed in necrotic muscle fibers [12], increased urinary PGDM is supposed to relate with abundance of necrotic muscle fibers.

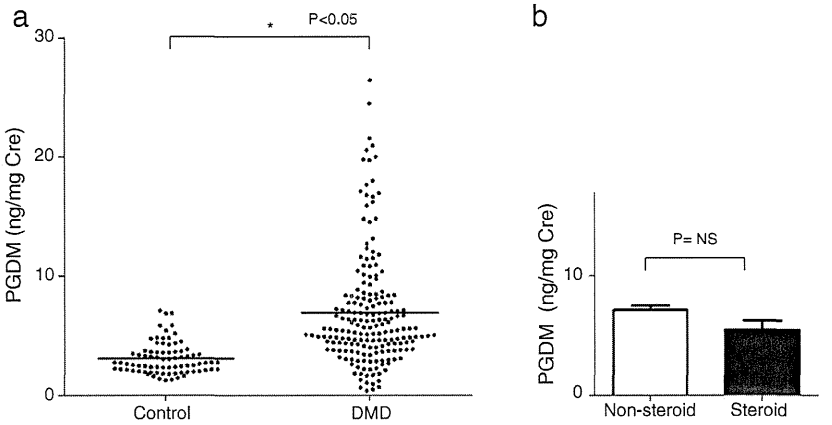

Fig. 2. Urinary tetranor PGDM in DMD patients and healthy children. a. Urinary tetranor PGDM concentration in DMD patients and healthy control children. Individual data points showing urinary tetranor PGDM concentration are represented by circles. In controls, the levels of tetranor PGDM were 3.08 ± 0.15 ng/mg creatinine (mean ± SE) (range, 1.23 to 7.08 ng/mg creatinine), while those were 6.90 ± 0.35 ng/mg creatinine (range, 0.38 to 26.46 ng/mg creatinine) in DMD patients. The mean concentration of tetranor PGDM in DMD patients was approximately 2.2-times higher than that in controls ($p < 0.0001$). The horizontal bars represent the mean. b. Effect of corticosteroid treatment on urinary tetranor PGDM concentration in DMD patients. The average urinary excretion of tetranor PGDM was 5.44 ± 0.81 ($n = 28$) and 7.15 ± 0.38 ($n = 163$) ng/mg creatinine in DMD patients with (Steroid) and without corticosteroid therapy (Non-steroid), respectively. The data are shown as mean + SE. Bars and horizontal lines represent mean and SE, respectively. There was no significant difference between patients receiving corticosteroid (Steroid) ($n = 28$) or not receiving (Non-steroid) ($n = 163$) corticosteroid treatment.

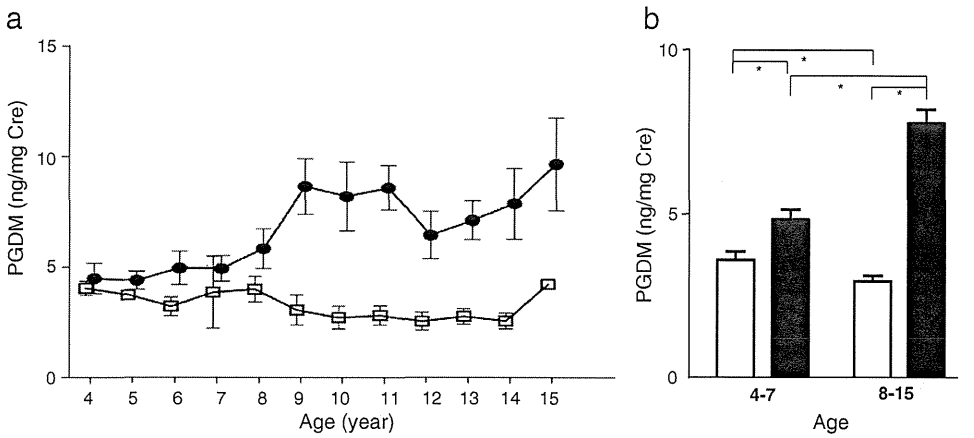

Fig. 3. Chronological changes of urinary tetranor PGDM. a. Chronological changes of mean levels of urinary tetranor PGDM. Mean levels of urinary tetranor PGDM are shown by age in 191 DMD samples (black circles) and 79 control samples (open boxes). The tetranor PGDM levels in DMD patients were higher than controls. Remarkably, they surged still higher from ages 8 to 9, the beginning of the non-ambulant stage, and stayed high level thereafter. However, the tetranor PGDM levels in controls were similar levels throughout the examination period. The data are shown as mean ± SE. b. Comparison of urinary tetranor PGDM concentrations in aged 4 to 7 and 8 to 15 groups. Mean concentration of urinary PGDM in aged 4–7 and 8–15 groups of DMD patients (black columns) and controls (open columns) are shown. In DMD urinary tetranor PGDM was significantly higher in the older age group (age 8–15) ($n = 140$) than in the younger age group (age 4–7) ($n = 51$) (7.69 ± 0.44 vs. 4.75 ± 0.32 ng/mg creatinine (mean ± SE) ($p < 0.05$)). In control, however, urinary tetranor PGDM was significantly lower in the older age group (age 8–15) ($n = 57$) than in the younger age group (age 4–7) ($n = 22$) (2.90 ± 0.17 vs. 3.55 ± 0.30 ng/mg creatinine (mean ± SE) ($p < 0.05$)). The data are represented as mean + SE. Asterisks mean significant difference ($p < 0.05$).

It has been demonstrated that creatinine excretion progressively decreases in parallel with muscle wasting in patients with Duchenne muscular dystrophy [19]. The apparent increase of tetranor PGDM (expressed as ng/mg creatinine) in the DMD patients (Fig. 2) was attributable, at least in part, to the decreased concentrations of creatinine excretion in these patients. Considering that urinary creatinine excretion could be a reliable index of muscle mass [20], urinary tetranor PGDM concentration expressed as ng/mg creatinine was considered to reflect a PGD_2 production in a certain amount of muscle mass. Namely, DMD patients are supposed to have higher HPGDS activity than controls in a certain volume of muscle. Ideally, tetranor PGDM concentrations would have been studied in 24 h urine samples, allowing them also to be expressed as total output per day and hence independent of creatinine concentration. However, it was not considered reasonable to perform 24 h urine collections in this patient population.

HPGDS is widely distributed in various human organs [21]. However, the remarkable increases in HPGDS in DMD boys are observed only in the skeletal muscle [12]. The other type of PGDS, lipocalin-type PGDS, is distributed in the heart, male genital organs, and the central nervous system [22]. Lipocalin-type PGDS is not increased in the DMD muscle. In *mdx* mice, a murine model of DMD, the urinary tetranor PGDM concentration was decreased by administration of an HPGDS inhibitor, HQL-79 [16]. These indicated that urinary tetranor PGDM in DMD is mainly produced by HPGDS-derived PGD_2.

Administration of corticosteroids has been reported to give some benefit to DMD patients [23,24]. The mechanism through which corticosteroids exert their action is still unclear [15]. It has been proposed that corticosteroids alleviate the dystrophy process through immunosuppression and reduction of inflammation [25] or that corticosteroids act directly on muscle fibers by stabilizing sarcolemma [26]. It was reported that corticosteroids suppress the biosynthesis of prostaglandins by suppression of their biosynthesis enzymes including phospholipase A_2 and cyclooxygenase [27]. Therefore, corticosteroids were supposed to decrease urinary tetranor PGDM excretion by suppression of prostaglandin synthesis. However, we found no significant difference in urinary tetranor PGDM concentrations between DMD patients with and without corticosteroid treatment (Fig. 2). This suggested that the benefits of corticosteroid administration are not mediated through PGD_2-related inflammation or that our treatment protocol (0.5 mg/kg on alternative days) is not enough to modulate PGDS. It needs further study to clarify this.

DMD is caused by a deficiency of dystrophin in skeletal muscle. The clinical time-course of DMD is well known [9], but the detailed pathogenesis of the progressive muscle wasting has not been elucidated. Muscle degeneration can be observed before birth [6], but the minimal disability stage occurs between ages 4 and 5 y. Mechanical injury to dystrophin deficient membranes is an important factor promoting dystrophic disease pathology but it does not fully explain DMD disease onset and progression. Aberrant intracellular signaling cascades, which regulate both inflammatory and immune processes, have been considered to contribute substantially to the degenerative process. Observations of upregulated inflammatory genes and activated immune cell infiltrates during critical disease stages in dystrophic muscle suggest that these inflammatory processes may play a critical role in initiating and exacerbating muscle wasting [28–32]. A major limitation in understanding the role of the inflammatory immune response in DMD is the absence of detailed time-course studies before, during, and after the onset of lesion development in the muscles of affected humans. It was remarkable that urinary tetranor PGDM concentrations changed chronologically, with a notable increase from the age of 8 y (Fig. 3a). Our findings are compatible with those of Okinaga et al. who showed HPGDS-positive hyalinated necrotic muscle fibers in all aged DMD patients but not in all younger patients [12]. Taken this into consideration, it was suggested that hyalinated fibers expressing HPGDS increase in skeletal muscles of aged DMD patients.

It has been suggested that cycles of degeneration and regeneration in dystrophic muscle eventually deplete satellite replacement cells (i.e., muscle stem cells) [8,33] and that, once the satellite cells are depleted, muscle regeneration ceases, promoting the progressive replacement of muscle tissue with adipose and fibrous connective tissues [34]. However, the mechanisms regulating the degeneration and regeneration cycles have not been clearly defined [9]. Ages 8 to 9 y when urinary tetranor PGDM surged corresponds to the time when the clinical disability changes from the minimal to the severe disability stage. It was supposed that the surge in production of PGD_2 may relate to this progression. The loss of ambulation was reported to manifest at a mean age of 10.3 y in a recent study on genetically confirmed DMD cases [2]. High plateau concentration of urinary tetranor PGDM corresponded to this non-ambulant stage. Our results suggest that PGD_2-mediated inflammation augments pathophysiology in the advanced stages of DMD. Therefore, chronological changes of urinary tetranor PGDM were considered to reflect clinical progression.

Inhibition of PGD_2 production has been proposed as a target of DMD treatment based on an animal study [16]. Administration of the HPGDS inhibitor HQL-79 was shown to decrease urinary tetranor PGDM concentrations and ameliorate muscle necrosis in *mdx* mice, DMD model mice [16]. Our results showing high production of PGD_2 in DMD provide a rationale for the administration of an HPGDS inhibitor to DMD patients. Recently, a cyclooxygenase inhibitor was shown to be effective in slowing the progression of muscular dystrophy in α-sarcoglycan-null mice [35]. Considering that PGD_2 is synthesized from PGH_2, a product of arachidonic acid generated by cyclooxygenase, inhibition of cyclooxygenase is another choice for the suppression of PGH_2, leading to a decrease in PGD_2. Aspirin has been shown to decrease urinary tetranor PGDM concentrations significantly [16], and to ameliorate muscle morphology in *mdx* mice [36]. So this common drug may also be useful for the treatment of DMD.

5. Conclusion

Urinary tetranor PGDM concentrations were increased in DMD patients and became higher with advancing age. It was indicated that PGD_2-mediated inflammation plays a role in the pathology of DMD. It was supposed that hyalinated fibers expressing HPGDS increase in older DMD patients.

List of abbreviations

DMD Duchenne muscular dystrophy
PG prostaglandin
HPGDS hematopoietic prostaglandin D synthase
tetranor PGDM 11,15-dioxo-9α-hydroxy-,2,3,4,5-tetranorprostan-1,20-dioic acid
tetranor PGEM 9,15-dioxo-11α-hydroxy-,2,3,4,5-tetranorprostan-1,20-dioic acid.

Acknowledgments

We thank all the participating families and the Happy Smile Club. We are grateful to Drs. Shinya Kamauchi and Kousuke Aritake (Department of Molecular Behavioral Biology, Osaka Bioscience Institute, Suita, Osaka, Japan) for their valuable suggestions. This work was supported by a Grant-in-Aid for Scientific Research (B), and a Grant-in-Aid for Exploratory Research from the Japan Society for the Promotion of Science, a Health and Labour Sciences Research Grant for Research on Psychiatric and Neurological Diseases and Mental Health, and a research grant for Nervous and Mental Disorders from the Ministry of Health, Labour, and Welfare, Japan.

References

[1] Takeshima Y, Yagi M, Okizuka Y, et al. Mutation spectrum of the dystrophin gene in 442 Duchenne/Becker muscular dystrophy cases from one Japanese referral center. J Hum Genet 2010;55:379–88.
[2] Magri F, Govoni A, D'Angelo MG, et al. Genotype and phenotype characterization in a large dystrophinopathic cohort with extended follow-up. J Neurol 2011;258:1610–23.
[3] Nishiyama A, Takeshima Y, Zhang Z, et al. Dystrophin nonsense mutations can generate alternative rescue transcripts in lymphocytes. Ann Hum Genet 2008;72:717–24.
[4] Desguerre I, Christov C, Mayer M, et al. Clinical heterogeneity of Duchenne muscular dystrophy (DMD): definition of sub-phenotypes and predictive criteria by long-term follow-up. PLoS One 2009;4:e4347.
[5] Sifringer M, Uhlenberg B, Lammel S, et al. Identification of transcripts from a subtraction library which might be responsible for the mild phenotype in an intrafamilially variable course of Duchenne muscular dystrophy. Hum Genet 2004;114:149–56.
[6] Brooke MH, Fenichel GM, Griggs RC, et al. Clinical investigation in Duchenne dystrophy: 2. Determination of the "power" of therapeutic trials based on the natural history. Muscle Nerve 1983;6:91–103.
[7] Mendell JR, Province MA, Moxley III RT, et al. Clinical investigation of Duchenne muscular dystrophy. A methodology for therapeutic trials based on natural history controls. Arch Neurol 1987;44:808–11.
[8] Bell CD, Conen PE. Histopathological changes in Duchenne muscular dystrophy. J Neurol Sci 1968;7:529–44.
[9] Evans NP, Misyak SA, Robertson JL, Bassaganya-Riera J, Grange RW. Dysregulated intracellular signaling and inflammatory gene expression during initial disease onset in Duchenne muscular dystrophy. Am J Phys Med Rehabil 2009;88:502–22.
[10] Urade Y, Ujihara M, Horiguchi Y, et al. Mast cells contain spleen-type prostaglandin D synthetase. J Biol Chem 1990;265:371–5.
[11] Urade Y, Hayaishi O. Prostaglandin D synthase: structure and function. Vitam Horm 2000;58:89–120.
[12] Okinaga T, Mohri I, Fujimura H, et al. Induction of hematopoietic prostaglandin D synthase in hyalinated necrotic muscle fibers: its implication in grouped necrosis. Acta Neuropathol 2002;104:377–84.
[13] Song WL, Wang M, Ricciotti E, et al. Tetranor PGDM, an abundant urinary metabolite reflects biosynthesis of prostaglandin D2 in mice and humans. J Biol Chem 2008;283:1179–88.
[14] Shinozawa T, Urade Y, Maruyama T, Watabe D. Tetranor PGDM analyses for the amyotrophic lateral sclerosis: positive and simple diagnosis and evaluation of drug effect. Biochem Biophys Res Commun 2011;415:539–44.
[15] Moxley III RT, Pandya S, Ciafaloni E, Fox DJ, Campbell K. Change in natural history of Duchenne muscular dystrophy with long-term corticosteroid treatment: implications for management. J Child Neurol 2010;25:1116–29.
[16] Mohri I, Aritake K, Taniguchi H, et al. Inhibition of prostaglandin D synthase suppresses muscular necrosis. Am J Pathol 2009;174:1735–44.
[17] Zhang Y, Zhang G, Clarke PA, et al. Simultaneous and high-throughput quantitation of urinary tetranor PGDM and tetranor PGEM by online SPE-LC–MS/MS as inflammatory biomarkers. J Mass Spectrom 2011;46:705–11.
[18] Higashi N, Mita H, Yamaguchi H, Fukutomi Y, Akiyama K, Taniguchi M. Urinary tetranor-PGDM concentrations in aspirin-intolerant asthma and anaphylaxis. J Allergy Clin Immunol 2012;129:557–9.
[19] Griggs RC, Forbes G, Moxley RT, Herr BE. The assessment of muscle mass in progressive neuromuscular disease. Neurology 1983;33:158–65.
[20] Wang ZM, Gallagher D, Nelson ME, Matthews DE, Heymsfield SB. Total-body skeletal muscle mass: evaluation of 24-h urinary creatinine excretion by computerized axial tomography. Am J Clin Nutr 1996;63:863–9.
[21] Kanaoka Y, Fujimori K, Kikuno R, Sakaguchi Y, Urade Y, Hayaishi O. Structure and chromosomal localization of human and mouse genes for hematopoietic prostaglandin D synthase. Conservation of the ancestral genomic structure of sigma-class glutathione S-transferase. Eur J Biochem 2000;267:3315–22.
[22] Smith WL, Urade Y, Jakobsson PJ. Enzymes of the cyclooxygenase pathways of prostanoid biosynthesis. Chem Rev 2011;111:5821–65.
[23] Manzur AY, Kuntzer T, Pike M, Swan A. Glucocorticoid corticosteroids for Duchenne muscular dystrophy.Cochrane Database Syst Rev 2008(1) [CD003725].
[24] Escolar DM, Hache LP, Clemens PR, et al. Randomized, blinded trial of weekend vs daily prednisone in Duchenne muscular dystrophy. Neurology 2011;77:444–52.
[25] Iannitti T, Capone S, Feder D, Palmieri B. Clinical use of immunosuppressants in Duchenne muscular dystrophy. J Clin Neuromuscul Dis 2010;12:1–21.
[26] Jacobs SC, Bootsma AL, Willems PW, Bar PR, Wokke JH. Prednisone can protect against exercise-induced muscle damage. J Neurol 1996;243:410–6.
[27] Masferrer JL, Seibert K, Zweifel B, Needleman P. Endogenous glucocorticoids regulate an inducible cyclooxygenase enzyme. Proc Natl Acad Sci U S A 1992;89:3917–21.
[28] Spencer MJ, Montecino-Rodriguez E, Dorshkind K, Tidball JG. Helper (CD4(+)) and cytotoxic (CD8(+)) T cells promote the pathology of dystrophin-deficient muscle. Clin Immunol 2001;98:235–43.
[29] Porter JD, Merriam AP, Leahy P, Gong B, Khanna S. Dissection of temporal gene expression signatures of affected and spared muscle groups in dystrophin-deficient (mdx) mice. Hum Mol Genet 2003;12:1813–21.
[30] Chen YW, Nagaraju K, Bakay M, et al. Early onset of inflammation and later involvement of TGFbeta in Duchenne muscular dystrophy. Neurology 2005;65:826–34.
[31] Pescatori M, Broccolini A, Minetti C, et al. Gene expression profiling in the early phases of DMD: a constant molecular signature characterizes DMD muscle from early postnatal life throughout disease progression. FASEB J 2007;21:1210–26.
[32] Lawler JM. Exacerbation of pathology by oxidative stress in respiratory and locomotor muscles with Duchenne muscular dystrophy. J Physiol 2011;589:2161–70.
[33] Webster C, Silberstein L, Hays AP, Blau HM. Fast muscle fibers are preferentially affected in Duchenne muscular dystrophy. Cell 1988;52:503–13.
[34] Collins CA, Morgan JE. Duchenne's muscular dystrophy: animal models used to investigate pathogenesis and develop therapeutic strategies. Int J Exp Pathol 2003;84:165–72.
[35] Sciorati C, Miglietta D, Buono R, et al. A dual acting compound releasing nitric oxide (NO) and ibuprofen, NCX 320, shows significant therapeutic effects in a mouse model of muscular dystrophy. Pharmacol Res 2011;64:210–7.
[36] Serra F, Quarta M, Canato M, et al. Inflammation in muscular dystrophy and the beneficial effects of non-steroidal anti-inflammatory drugs. Muscle Nerve 2012;46:773–84.

Journal of Molecular and Cellular Cardiology 59 (2013) 76–85

Contents lists available at SciVerse ScienceDirect

Journal of Molecular and Cellular Cardiology

journal homepage: www.elsevier.com/locate/yjmcc

Original article

Global metabolomic analysis of heart tissue in a hamster model for dilated cardiomyopathy

Keiko Maekawa [a,1], Akiyoshi Hirayama [b,1], Yuko Iwata [c,1], Yoko Tajima [a], Tomoko Nishimaki-Mogami [a], Shoko Sugawara [b], Noriko Ueno [a], Hiroshi Abe [b], Masaki Ishikawa [a], Mayumi Murayama [a], Yumiko Matsuzawa [a], Hiroki Nakanishi [a,d], Kazutaka Ikeda [b], Makoto Arita [a,e], Ryo Taguchi [a,f], Naoto Minamino [c], Shigeo Wakabayashi [c], Tomoyoshi Soga [b,*,1], Yoshiro Saito [a,**,1]

[a] Project Team for Disease Metabolomics, National Institute of Health Sciences, Tokyo 158-8501, Japan
[b] Institute for Advanced Biosciences, Keio University, Tsuruoka, Yamagata 997-0052, Japan
[c] National Cerebral and Cardiovascular Center Research Institute, Suita, Osaka 565-8565, Japan
[d] Bioscience and Research Center, Akita University, Akita 010-8543, Japan
[e] Department of Health Chemistry, Graduate School of Pharmaceutical Sciences, University of Tokyo, Tokyo 113-0033, Japan
[f] College of Life and Health Sciences, Chubu University, Kasugai, Aichi 487-8501, Japan

ARTICLE INFO

Article history:
Received 19 September 2012
Received in revised form 8 January 2013
Accepted 6 February 2013
Available online 20 February 2013

Keywords:
Dilated cardiomyopathy
Hamster model
Metabolomics
Oxidative stress
Phospholipid alteration

ABSTRACT

Dilated cardiomyopathy (DCM), a common cause of heart failure, is characterized by cardiac dilation and reduced left ventricular ejection fraction, but the underlying mechanisms remain unclear. To investigate the mechanistic basis, we performed global metabolomic analysis of myocardial tissues from the left ventricles of J2N-k cardiomyopathic hamsters. This model exhibits symptoms similar to those of human DCM, owing to the deletion of the δ-sarcoglycan gene. Charged and lipid metabolites were measured by capillary electrophoresis mass spectrometry (MS) and liquid chromatography MS(/MS), respectively, and J2N-k hamsters were compared with J2N-n healthy controls at 4 (presymptomatic phase) and 16 weeks (symptomatic) of age. Disturbances in membrane phospholipid homeostasis were initiated during the presymptomatic phase. Significantly different levels of charged metabolites, occurring mainly in the symptomatic phase, were mapped to primary metabolic pathways. Reduced levels of metabolites in glycolysis, the pentose phosphate pathway, and the tricarboxylic acid cycle, together with large decreases in major triacylglycerol levels, suggested that decreased energy production leads to cardiac contractile dysfunction in the symptomatic phase. A mild reduction in glutathione and a compensatory increase in ophthalmate levels suggest increased oxidative stress in diseased tissues, which was confirmed by histochemical staining. Increased levels of 4 eicosanoids, including prostaglandin (PG) E_2 and 6-keto-$PGF_{1\alpha}$, in the symptomatic phase suggested activation of the protective response pathways. These results provide mechanistic insights into DCM pathogenesis and may help identify new targets for therapeutic intervention and diagnosis.

1. Introduction

Dilated cardiomyopathy (DCM), a common cause of heart failure and a prevalent cardiomyopathy [1], is characterized by left ventricular dilation, impaired cardiac pump function, and a thin cardiac wall, which result in severe contractile dysfunction. β-Blockers constitute a common treatment [2], but severely affected patients may undergo heart transplantation or implantation of left ventricular assist devices. While the underlying etiological factors remain largely unknown, and both familial and non-familial factors are associated with DCM, some proposed disease mechanisms include coronary artery disease, genetic mutation, and viral infection [3]. Mutations in sarcomeric and cytoskeletal genes cause hypertrophic and dilated cardiomyopathies, respectively [4]. Some familial DCM cases are caused by mutations in genes encoding components of the dystrophin–glycoprotein complex (DGC), which spans the sarcolemma linking the extracellular matrix and cytoskeleton and provides mechanical strength for contraction [5]. Mutations in dystrophin, a major cytoskeletal component of the DGC, lead to a high incidence of X-linked DCM in patients with

* Correspondence to: T. Soga, Institute for Advanced Biosciences, Keio University, 246-2 Mizukami, Kakuganji, Tsuruoka, Yamagata 997-0052, Japan. Tel.: +81 235 29 0528; fax: +81 235 29 0574.
** Correspondence to: Y. Saito, Project Team for Disease Metabolomics, National Institute of Health Sciences, 1-18-1 Kamiyoga, Setagaya-ku, Tokyo 158-8501, Japan. Tel.: +81 3 3700 9528; fax: +81 3 3700 9788.
E-mail addresses: soga@sfc.keio.ac.jp (T. Soga), yoshiro@nihs.go.jp (Y. Saito).
[1] Contributed equally to this work.

0022-2828/$ – see front matter © 2013 Elsevier Ltd. All rights reserved.
http://dx.doi.org/10.1016/j.yjmcc.2013.02.008

Duchenne or Becker muscular dystrophy. Mutations in other DGC genes, including *δ-sarcoglycan*, are also associated with human DCM [1].

Oxidative stress is also reported to be involved in DCM pathogenesis. Patients with DCM exhibit increased plasma glutathione levels and lipid peroxidation products such as malondialdehyde [6], and total plasma peroxide levels are inversely correlated with the cardiac ejection fraction [7]. However, a contrasting study found that human left ventricular DCM tissue showed normal glutathione peroxidase and superoxide dismutase activities and malondialdehyde levels similar to those found in healthy control tissue [8]. Thus, the role of oxidative stress in DCM pathogenesis remains to be elucidated.

Animal models with a pathophysiology similar to human DCM are useful for investigating pathogenic mechanisms. A J2N-k DCM hamster and J2N-n control line were established by repeated sib mating of J2N(N8), produced by cross-breeding BIO14.6 cardiomyopathic and normal golden hamsters [9]. J2N-k hamsters are deficient in δ-sarcoglycan and are an animal model of human limb-girdle muscular dystrophy–associated cardiomyopathy. They begin showing heart tissue fibrosis and exhibit moderate cardiac dysfunction at 8–9 weeks of age. At 20 weeks, J2N-k hamsters exhibit considerable fibrosis, a reduced number of cardiomyocytes, and hypertrophic changes in the remaining cardiomyocytes; no such changes occur in J2N-n heart tissues [9]. Accordingly, the life span of J2N-k hamsters (ca. 298 days) is much shorter than that of J2N-n hamsters (ca. 788 days). Besides the *δ-sarcoglycan* gene, J2N-k and J2N-n hamsters have very similar genetic backgrounds. Since mutations in *δ-sarcoglycan* are also detected in DCM patients, J2N-k hamsters are an ideal DCM disease model.

To gain an insight into the DCM in metabolic pathway basis, we performed global metabolomic analysis of myocardial tissues from the left ventricles of J2N-k and J2N-n hamsters. Capillary electrophoresis-time-of-flight mass spectrometry (CE-TOFMS) [10] and liquid chromatography (LC)-TOFMS or triple quadrupole MS/MS were used to measure levels of charged (e.g., amino acids) and lipid (e.g., phospholipids) metabolites, respectively. We identified significant changes in several metabolite levels in age-matched J2N-k and J2N-n hamsters.

2. Methods

2.1. Animals

Male 3- and 15-week-old J2N-k cardiomyopathic hamsters and age-matched J2N-n controls were purchased from Nihon SLC Inc. (Hamamatsu, Japan). All animals were maintained in a specific pathogen-free facility under controlled conditions (20–24 °C and 40–70% humidity) with a 12-h light cycle and were given free access to standard laboratory rat chow (MF, Oriental Yeast, Tokyo, Japan) and tap water. After 1 week of habituation, 4- and 16-week-old animals were anesthetized by intraperitoneal injection of pentobarbital (Dainippon Sumitomo Pharma, Osaka, Japan) at a dose of 50 mg/kg, and the left ventricle was excised. The isolated tissue was processed for either histological analysis (N = 4) or for metabolomic and western blot analysis (N = 7). For metabolomic analysis, tissue was randomly divided into 2 samples and minced on ice to measure charged and lipid metabolites. The tissue samples were weighed and snap frozen in liquid nitrogen before being stored at −80 °C. All animal experiments were performed in accordance with the Guide for the Care and Use of Laboratory Animals published by the US National Institutes of Health (NIH Publication No. 85-23, revised 1996) and the Guidelines for Animal Experimentation and under the control of the Ethics Committee of Animal Care and Experimentation of the National Cerebral and Cardiovascular Center, Japan (Approval number, 12056).

2.2. Echocardiography and histochemical staining

Cardiac function was assessed by echocardiography measurements as shown in the supplementary information. Following this procedure, J2N-k and J2N-n hamsters were sacrificed as described above, and ventricle tissue (from both hamster lines) was processed for Masson's trichrome staining to detect fibrosis, 4-hydroxynonenal (4-HNE) staining to estimate lipid peroxidation [11], and dihydroethidium (DHE) staining to approximate superoxide production [12] as described in the supplementary information.

2.3. Metabolite extraction and quantification

Detailed information regarding the extraction and quantification of charged and lipid metabolites has been provided in the supplementary information. Briefly, charged metabolites were extracted by homogenizing myocardial tissue in methanol and subjected to CE-TOFMS, as previously described [10,13,14]. Lipid metabolite extraction was performed using the Bligh and Dyer method [15] with minor modifications. Lower organic and upper aqueous layers were analyzed by LC-TOFMS and LC-MS/MS for phospholipids/sphingolipids/triacylglycerols and oxidative fatty acids, respectively. Structural analysis of phospholipids (PLs) and sphingomyelins (SMs) was performed as previously described [16].

2.4. Data analysis

Datasets obtained from CE-TOFMS were processed using our proprietary software, MasterHands [17] as shown in the supplementary information. Hydrophilic metabolite concentrations have been provided as the amount of metabolite (μmol) per gram of tissue.

LC-TOFMS data were processed using the 2DICAL software (Mitsui Knowledge Industry, Tokyo, Japan) [18] as described in the supplementary information. Extracted ion peaks were normalized using internal standards (ISs). Metabolites eluting from 0.1 to 37.5 min and from 37.5 to 60 min for LC were normalized to 1, 2-dipalmitoyl-[$^2H_6$]-sn-glycero-3-phosphocholine (16:0-16:0PC-d6; Larodan Fine Chemicals, Malmo, Sweden) and 1,2-caprylin-3-linolein, respectively. Some oxidative fatty acids were quantified using commercially available standards.

2.5. Statistical and multiple classification analyses

Student's *t*-test was used for two-class comparisons between J2N-n and J2N-k at each growth stage (4 and 16 weeks), and $p<0.05$ was deemed as statistically significant. The multiple testing correction was not applied since metabolite levels are not exclusive but rather related with each other, and we focused on revealing overall metabolic changes (such as pathways or metabolite groups) in the cardiomyocytes from J2N-k hamsters compared to J2N-n cardiomyocytes. In addition, data were imported into the SIMCA-P+ software (Version 12.0; Umetrics, Umeå, Sweden), pareto-scaled, and subjected to principal component analysis (PCA; short explanation is provided in the supplementary information). Cluster analysis and heatmap representations were obtained using the Spotfire software (Version 7.1; TIBCO, MA, USA).

3. Results

3.1. Cardiac function and pathophysiology of J2N-n and J2N-k hamsters

In this study, the 4- and 16-weeks of ages were selected as DCM presymptomatic and symptomatic phases for J2N-k (and its control J2N-n) hamsters according to the previous paper [9]. First, we examined cardiac function of both hamsters at these time points. Echocardiograph measurements of J2N-k hamsters at 16 weeks revealed a significant increase in the internal diameter of the left ventricle (LVID) during both diastolic and systolic states; however, this

Table 1
Summary of echocardiographic analysis.

		4 weeks	4 weeks	16 weeks	16 weeks	
		J2N-n	J2N-k	J2N-n	J2N-k	*p* values
LVIDd	mm	3.10 ± 0.05	2.89 ± 0.23	3.80 ± 0.36	5.07 ± 0.26	0.0291*
LVIDs	mm	1.49 ± 0.10	1.21 ± 0.20	2.06 ± 0.18	3.64 ± 0.21	0.0013**
LVPWd	mm	1.85 ± 0.18	1.82 ± 0.31	2.09 ± 0.30	1.77 ± 0.09	0.3487
LVPWs	mm	2.22 ± 0.11	2.08 ± 0.22	2.28 ± 0.27	1.95 ± 0.13	0.3285
EF	%	77.64 ± 1.43	83.68 ± 3.07	77.64 ± 1.44	54.46 ± 1.04	<0.0001***
FS	%	51.80 ± 3.53	58.41 ± 5.63	45.62 ± 1.41	28.35 ± 0.60	<0.0001***
LV VOLd	μL	38.03 ± 1.46	32.81 ± 6.57	64.50 ± 14.69	123.70 ± 15.58	0.0327*
LV VOLs	μL	6.13 ± 1.08	4.01 ± 1.53	14.31 ± 2.94	56.69 ± 8.27	0.0029**

LVIDd, left ventricular internal diameter in diastole; LVIDs, left ventricular internal diameter in systole; LVPWd, left ventricular posterior wall in diastole; LVPWs, left ventricular posterior wall in systole; EF, ejection fraction; FS, fractional shortening (given by (LVIDd-LVIDs)/LVIDd × 100); LV VOLd, left ventricular volume in diastole; LV VOLs, left ventricular volume in systole. *p* values are analyzed between 16 week-old J2N-k and J2N-n hamsters. In 4 week-old hamsters, the *p* values are not significant.
* $p<0.05$.
** $p<0.005$.
*** $p<0.0001$.

was not observed at 4 weeks of age (Table 1). In addition, markedly reduced ejection fractions and fractional shortening were revealed at 16 weeks (Table 1 and Supplementary Fig. 1). Extensive fibrosis was observed in J2N-k hamsters at 16 weeks (compared to the J2N-n) by Masson's trichrome staining (Supplementary Fig. 2). No fibrosis was observed at 4 weeks. Thus, no obvious pathophysiological change was observed at 4 weeks, although DCM was obvious at 16 weeks in J2N-k hamsters.

3.2. Profiling of charged metabolites measured by CE-TOFMS

Charged metabolite levels were quantified absolutely using standard chemicals for each metabolite, whereas lipid metabolite levels were quantified relatively as ratios of ion counts (peak height) of each metabolite to those of the internal standard, with the exception of some oxidative fatty acids. Therefore, statistical analyses of charged and lipid metabolites were carried out separately.

A total of 180 charged metabolites were identified and quantified by the CE-TOFMS method (Supplementary Table 2). Using a whole dataset of quantified metabolites, we performed a PCA (Supplementary Fig. 3) in order to understand the similarities/dissimilarities of 4 animal groups regarding variations in metabolite levels. From the PCA score plot, DCM and control hamsters at 16 weeks (but not at 4 weeks) were separated in the first 2 principal components. This analysis indicates that the profiles of charged metabolites reflect the metabolic differences caused by disease progression.

Next, Student's *t*-test was used to examine DCM-associated metabolic changes (Supplementary Table 2). Using a *p*-value threshold of 0.01 to generate a heatmap (Fig. 1A), the levels of 15 metabolites were found to differ between J2N-k and J2N-n hamsters at 4 weeks; specifically, the level of 12 metabolites increased and 3 metabolites decreased in J2N-k hamsters. At the symptomatic phase (16 weeks), 62 metabolites were detected at different levels ($p<0.01$) in J2N-k and J2N-n hamsters (Fig. 1B), including 10 metabolites that also showed significant differences in the presymptomatic phase (4 weeks; 2-aminobutyrate (2-AB), citrulline, guanidinoacetate, hypotaurine, methionine, *N*-acetylaspartate, ophthalmate, ornithine, threonine, and trigonelline). Of the 62 metabolites showing variation, the levels of 26 increased and 36 decreased in the J2N-k hamsters. Most of these metabolites are components of primary metabolic pathways such as glycolysis, the pentose phosphate pathway, the tricarboxylic acid (TCA) cycle, the glutathione biosynthesis pathway, and the urea cycle.

3.3. Energy metabolism

J2N-k myocardial tissues from 16-week-old animals exhibited changes in the levels of metabolic intermediates involved in energy metabolism. The concentrations of several intermediates involved in glycolysis, such as glucose 6-phopshate (G6P; levels of J2N-k/J2N-n = 0.5-fold, $p=5.9\times10^{-5}$), dihydroxyacetone phosphate (DHAP; 0.6-fold, $p=1.4\times10^{-3}$), and acetyl CoA (0.3-fold, $p=1.1\times10^{-5}$), were significantly reduced at 16 weeks but not at 4 weeks (Fig. 2).

Significantly decreased levels of the TCA cycle intermediates, isocitrate (0.6-fold, $p=1.5\times10^{-6}$) and malate (0.7-fold, $p=2.5\times10^{-3}$), were also observed in myocardial tissues from 16-week-old J2N-k hamsters. Decreased protein levels of aconitase 2, which catalyzes citrate to isocitrate via *cis*-aconitate, were observed at 16 weeks in the J2N-k, suggesting decreased TCA cycle activity (Supplementary Fig. 4). These results suggest that the levels of metabolites involved in glycolysis and the TCA cycle energy pathways are attenuated in J2N-k cardiomyopathic tissue during the symptomatic phase.

3.4. Glutathione biosynthesis pathway

The ophthalmate and 2-AB levels were significantly higher in J2N-k myocardial tissues than in J2N-n control tissue at both the presymptomatic (1.4-fold, $p=2.6\times10^{-3}$; 2.2-fold, $p=6.9\times10^{-5}$, respectively) and symptomatic (2.3-fold, $p=3.9\times10^{-7}$; 4.2-fold, $p=2.2\times10^{-9}$, respectively) phases (Fig. 3). 2-AB is metabolized to ophthalmate via γ-Glu-2-AB through a 2-step reaction and then catalyzed sequentially by γ-glutamylcysteine synthetase and glutathione synthetase [10]. In contrast, γ-Glu-Cys and glutathione (GSH) concentrations are decreased at 16 weeks (0.2-fold, $p=7.9\times10^{-3}$; 0.8-fold, $p=2.0\times10^{-2}$, respectively). These data suggest that upregulation of the GSH biosynthetic pathway is associated with DCM progression. Consistent with this observation, intracellular levels of glycine (1.3-fold, $p=1.2\times10^{-5}$), methionine (1.3-fold, $p=2.9\times10^{-5}$), and *S*-adenosylhomocysteine (SAH; 1.2-fold, $p=2.4\times10^{-2}$) were elevated in J2N-k hamsters at 16 weeks. In contrast, *S*-adenosylmethionine (SAM; 0.9-fold, $p=3.2\times10^{-2}$) levels were reduced at the symptomatic-phase in J2N-k hamsters.

Taurine levels did not differ significantly between the 2 genotypes, although increased concentrations of its precursor, hypotaurine, were observed in J2N-k hamsters at both 4 weeks (1.6-fold, $p=6.9\times10^{-5}$) and 16 weeks (3.4-fold, $p=1.6\times10^{-9}$).

3.5. Urea cycle

The levels of most urea cycle intermediates significantly differed between myocardial tissues from J2N-k and J2N-n at 16 weeks (Fig. 4). The levels of arginine (0.7-fold, $p=3.2\times10^{-5}$), citrulline (0.6-fold, $p=2.0\times10^{-5}$), and argininosuccinate (0.4-fold, $p=6.3\times10^{-4}$) were significantly reduced in J2N-k hamsters. In contrast, ornithine levels (1.8-fold, $p=8.2\times10^{-8}$) were significantly increased. At 4 weeks, a

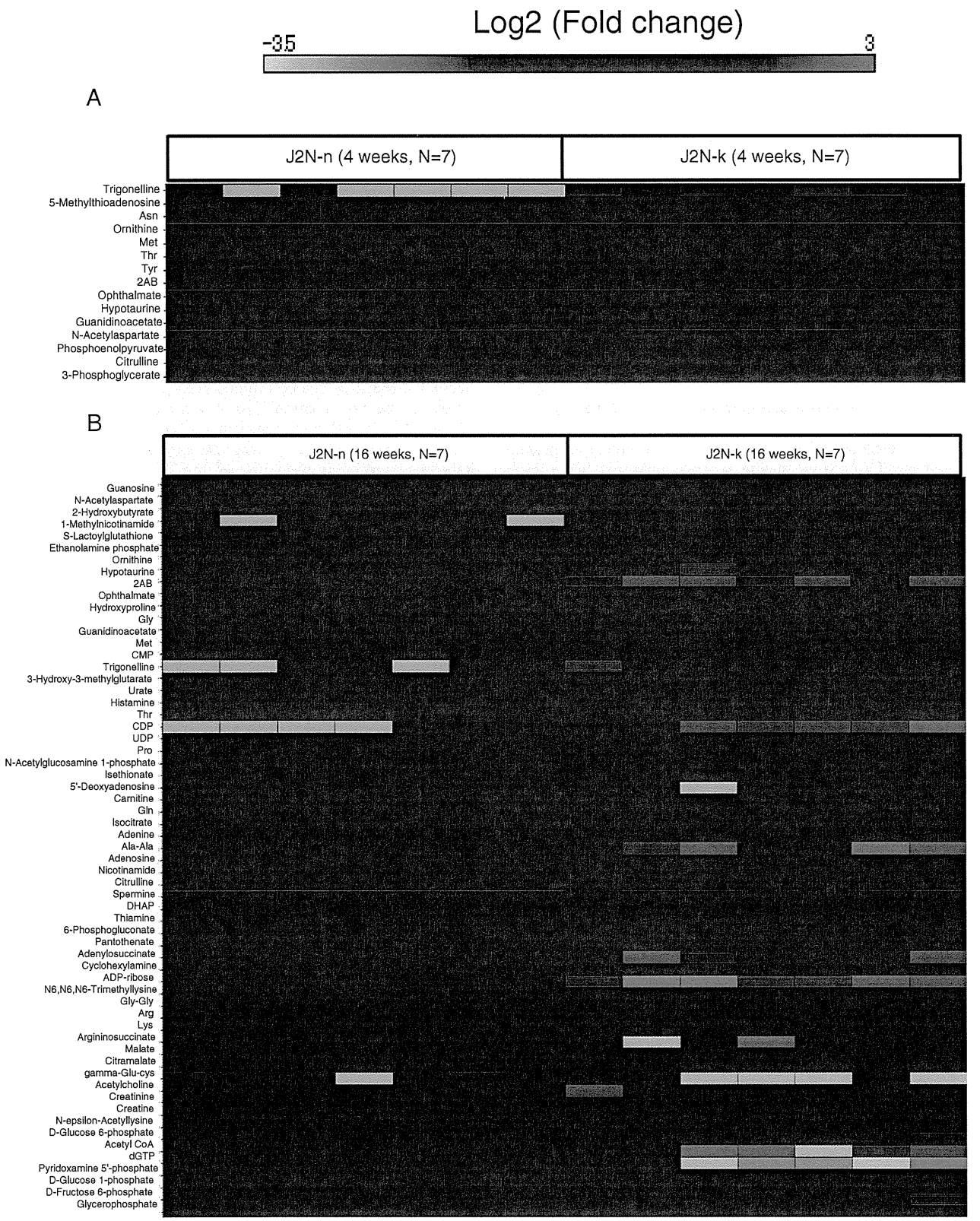

Fig. 1. Heatmap showing charged metabolites in myocardial tissues from J2N-n and J2N-k hamsters at (A) 4 weeks and (B) 16 weeks ($n=7$ in all groups). Fold changes in the amounts of each metabolite in individual J2N-k samples, relative to the average amounts in J2N-n at either 4 or 16 weeks are represented as the log2 ratio. Light gray cells indicate that metabolites were not detected in those samples. Fifteen (at 4 weeks) and sixty-two (at 16 weeks) charged metabolites that showed different levels ($p<0.01$) at each time point are shown, excluding Glu–Glu at 16 weeks, which was not detected in all J2N-n samples.

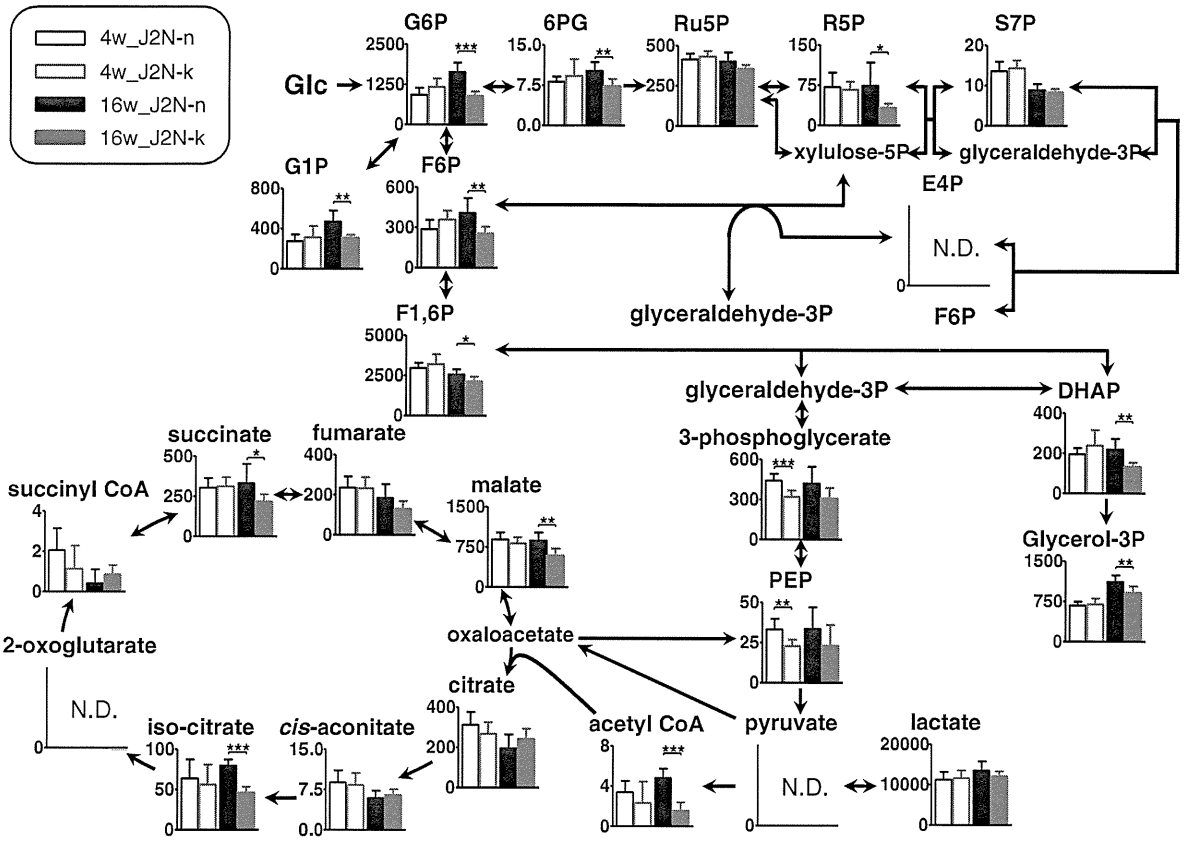

Fig. 2. Metabolome pathway map of quantified charged metabolites, including components of the glycolytic pathway, pentose phosphate pathway, and TCA cycle in J2N-n and J2N-k hamsters at 4 and 16 weeks (4w and 16w). The columns represent average concentrations (nmol/g tissue), and the error bars indicate SD. *$p<0.05$; **$p<0.01$; ***$p<0.001$; and N.D., not detected.

significant increase in ornithine levels (1.4-fold, $p=2.3\times10^{-4}$) and a decrease in citrulline levels (0.7-fold, $p=1.1\times10^{-3}$) were also observed in J2N-k hamsters.

3.6. Profiling of lipid metabolites measured by LC-TOFMS

LC-TOFMS detected 1173 peaks and 277 peaks in the positive and negative ion modes, respectively. Relative quantification of the identified metabolites is shown in Supplementary Table 3.

Next, the data were processed for PCA. In the positive ion mode, the 1173 peaks (including unidentified metabolites) were divided into 2 groups on the basis of their retention time (RT): 0.1–37.5 min RT (671 peaks; containing lysophospholipids [lysoPLs], diacylglycerols [DAGs], PLs, SMs, and ceramides [Cers]) and 37.5–60 min RT (502 peaks; containing triacylglycerols [TAGs] and cholesterol esters [ChEs]; Supplementary Fig. 5). PCA was performed separately for each group since PLs and TAGs are the 2 major classes of lipid metabolites in this mode (Supplementary Fig. 6). Distinct clustering of metabolites among the 4 groups (i.e., 4- or 16-week-old J2N-n and J2N-k hamsters) was observed in the data obtained using both positive (0.1–37.5 min RT; Supplementary Fig. 6A) and negative ion modes (data not shown). In contrast, for the second group of metabolites identified in the positive ion mode (37.5–60 min RT), poor discrimination was obtained between all tissue samples (from 4- and 16-week-old J2N-k and J2N-n hamsters) (Supplementary Fig. 6B). These results suggest that the lipid metabolites that were eluted from 0.1 to 37.5 min include candidates for identifying DCM and healthy tissues, even in the presymptomatic phase (4 weeks). Using a p-value threshold of 0.01 for the heatmap, the levels of 34 and 68 metabolites were found to differ between J2N-n and J2N-k hamsters at 4 and 16 weeks, respectively, with 15 overlapping metabolites (Fig. 5).

3.7. Myocardial lipid levels are significantly different in J2N-k and J2N-n tissues

PLs are important components of heart membranes. When focusing on phosphatidylcholine (PC), the levels of many species, most of which contained unsaturated fatty acids, increased in J2N-k compared with J2N-n at the presymptomatic phase (4 weeks). Some of these PC species remained upregulated in the symptomatic phase (16 weeks) (Fig. 5, Supplementary Table 3), including 18:0/20:4PC (1.4-fold, $p=5.4\times10^{-4}$; 1.6-fold, $p=2.0\times10^{-5}$; at 4 and 16 weeks, respectively) and 18:0/22:6PC (1.7-fold, $p=7.0\times10^{-5}$ and 1.7-fold, $p=2.0\times10^{-5}$; at 4 and 16 weeks, respectively). In contrast, levels of several PC species containing linoleic acid (18:2), such as 18:2/18:2PC (0.8-fold, $p=9.4\times10^{-3}$), were reduced at 16 weeks. As for lyso species, a significant increase in the level of 18:0 lyso PC (LPC; 1.4-fold, $p=9.5\times10^{-4}$) was observed in J2N-k at 16 weeks but not at 4 weeks.

Regarding phosphatidylethanolamine (PE) and plasmalogen PE (pPE), the levels of several species containing 22:5 and 22:6 (docosahexaenoic acid, DHA), such as 18:0/22:6PE (1.3-fold, $p=6.1\times10^{-3}$), increased in J2N-k compared with J2N-n hamsters at 4 weeks, although their increase was almost diminished at 16 weeks. At 16 weeks, many species (11 PEs and 8 pPEs) were decreased in J2N-k tissues (Fig. 5, Supplementary Table 3), although 3 PE and 2 pPE species were increased in J2N-k tissues. Notably, species containing linoleic acid (18:2) or eicosapentaenoic acid (EPA; 20:5),